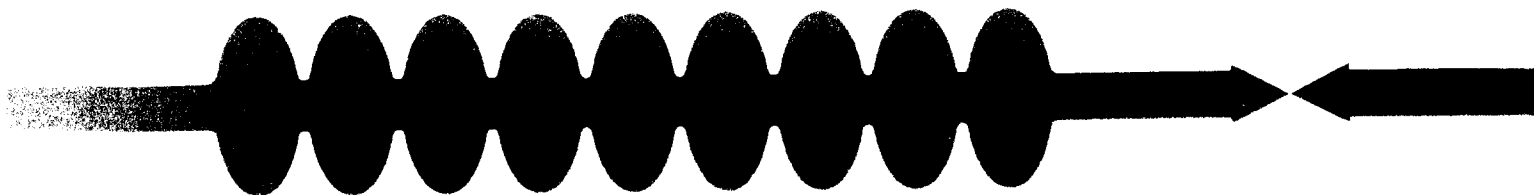


LL



TESLA - COLLABORATION

Contributions to the CEC/ICMC '95

July 17 - 21, 1995 in Columbus, Ohio

SCAN-9512010



CERN LIBRARIES, GENEVA

SW 9549



August 1995, TESLA 95-21

A NOVEL ROTATING TEMPERATURE AND RADIATION MAPPING SYSTEM IN SUPERFLUID He & ITS SUCCESSFUL DIAGNOSTICS

Q. S. Shu¹, T. Junquera², A. Caruette², G. Deppe¹, M. Fouaidy²
W-D. Moeller¹, M. Pekeler¹, D. Proch¹, D. Renken¹, C. Stolzenburg¹

¹Deutsches Elektronen-Synchrotron (DESY)
Notkestrasse 85, 22607 Hamburg, Germany

²Institute of Nuclear Physics
(CNRS - IN2P3) 91406 ORSAY cedex, France

ABSTRACT

An novel rotating temperature and radiation mapping system in He II has been developed to investigate field emission (FE) & thermal breakdown (TB) in TESLA 9-cell SRF cavities. More than 10,000 spots on a cavity surface can be analyzed in one turn with 5° stepping. 150 special surface scanning thermometers have been developed to measure surface temperature in He II. 32 photodiodes are employed to study the X-rays induced by FE electrons. Each rotating arm holds 14 thermometers and 4 photodiodes. A unique driving and suspension system is designed to gently turn the 9 arms around the cavity and uniformly press the thermometers against cavity surfaces. A moving adapter device (pancakes) is designed for rotating a large number of electronic cables which become inflexible in superfluid He.

The T-R mapping system has successfully detected and diagnosed serious problems caused by FE and TB, and has played a significant role in cavity processing.

INTRODUCTION

Main Obstacles of High Gradient Cavities

The field emission (FE) and thermal breakdown (TB) are still the main obstacles preventing SRF cavities from confidently reaching $E_{acc} = 25$ MV/m (TESLA's goal) from existing operating levels of 5-10 MV/m^{1,2,3}. Most of the FE sources and TB defects on the inner RF surfaces of cavities were found to be submicro-sizes^{4,5} and activated only at high RF fields while cavities are in a superconducting state. It is impossible to directly observe the FE and TB through inner surface of cavities during RF operation. Therefore, the main approach to understanding the FE and TB of cavities is to study the hot spots and X-rays (induced by impacting FE electrons) generated on the cavity surfaces during RF operation.

DESY's Rotating T-R Mapping System

Various temperature (T) mapping and X-ray (R) mapping systems have been developed at many laboratories around the world^{3,4,6,7,8}. The systems can be classified

into two categories: (1) Fixed Mapping - thermometers or photodiodes are fixed on the surfaces of cavity. (2) Rotating Mapping - thermometers or photodiodes are rotating against the surfaces of cavity.

The Rotating T-R mapping system developed at DESY for TESLA 9-cell cavities combines measurements of T & R and employs special rotating scanning thermometers which we developed at INP Orsay.

Advantages.

(1) Greatly reduce the number of sensors: The DESY T-R mapping analyzes 10,000 spots on cavity surface using only 116 scanning thermometers. A system using fixed thermometers would require 10,000 thermometers to analyse the same spots on cavity.

(2) Once an area is suspected, the sensors in DESY mapping system can be relocated to the suspect location during cryogenic-RF operation for additional analysis.

(3) The mapping combines T-R diagnostic system to give information on both heating and x-rays for understanding the dynamic progress of cavity processing.

Challenges.

(1) Fixed contacts and use of grease as bounding agent to enhance thermal contact between thermometer and surface being measured are essential to reach a high efficiency (particularly, in the case of He II). To a rotating system, neither fixed contact nor grease can be applied. New type of thermometers is needed⁹.

(2) Due to TESLA cavity structure, thermometers can not reach the high risk areas of FE at cavity irises. A combined measurement of T & R is required.

(3) The TESLA cavity has 9 cells (the largest cell number for low frequency cavities) with complex surface curves. The space of cavity test cryostat is tightly constrained. Assuring satisfaction of 3-dimension tolerances at all moving contact points is a challenge.

(4) To rotate a large number of measuring cables in He II while the mapping turns.

(5) A fast data acquisition system is also needed to trace the dynamic progress.

We have overcome the above challenges and developed the rotating T-R mapping system. Since December 1994, the system has been successfully employed in diagnostic tests and played a significant role in cavity processing¹⁰.

TECHNOLOGIES DEVELOPMENT

Surface scanning Thermometer and Photodiode

The surface thermometer design as shown in Figure 1(A) is very close to the model developed earlier for the CERN's SRF cavity project by INP Orsay^{10,11,12}. The sensitive part is an Allen-Bradley carbon resistor (100 Ohm, 1/8 W) housed in a silver block with a sensor tip of 1 mm diameter for the thermal contact to the external surface of the cavity. This housing is thermally insulated against the surrounding He II by an epoxy envelope (Stycast) moulded around the silver block and into a bronze piece which allows the sensor

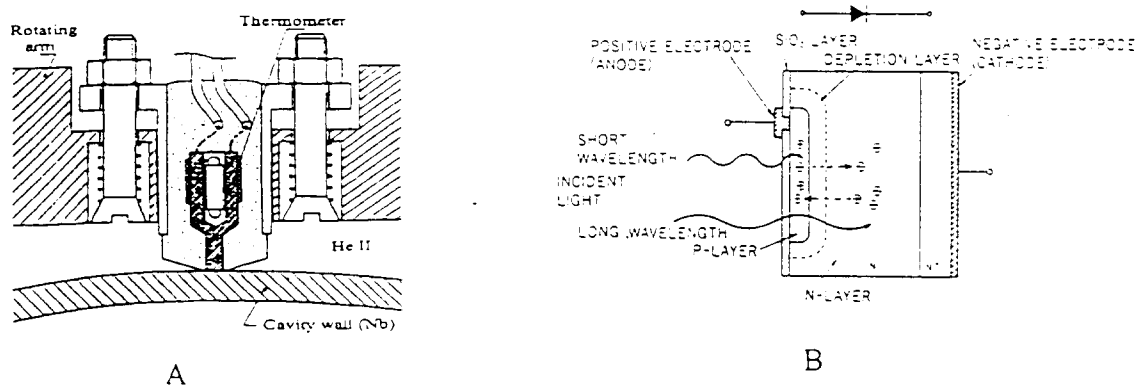


Figure 1 (A) Cross section of a HeII surface scanning thermometer. (B) cross section of a photodiode

to be mounted in the rotating thermometric arm. The thermometers tip must present a good contact with the cavity wall when scanning. Each thermometer has two independent manganin wires thermally anchored to the silver block with ~ 15 cm free length for connecting to each cell board (14 thermometers).

The complementary calibration test was performed by mounting the thermometers in the real operating conditions of the scanning device at different spring pressures and heating flux at He II and subcooled He (2.3K and one bar). The detailed results are presented in another paper⁹. In the case of He II, the efficiency is heater power dependant.

The commercial PIN silicon/S 1223-01 photodiodes are used as x-ray detectors in the mapping because of its small size (3mm x ϕ 10 mm) and its ultra-fast response. A simplified photodiode cross-section is shown in Figure 1(B).

Rotating T-R Arms

As shown in Fig 2, 14 thermometers and 4 photodiodes are mounted in each arm which is precisely machined to have the same curved surfaces as the cavity cell. Due to the reinforced structure of TESLA cavity, the thermometers can not directly touch the surfaces of the cavity iris. Considering the electrical fields reach maximum at the iris, 4 photodiodes are located in the end of each arm to monitor FE induced X-rays while 14 thermometers are used to monitor the temperatures in the entire region between the irises of each cell¹³. Two springs located inside two holes in the body of the rotating arm are used to adjust the contact pressure. A printed electron board is mounted on the side of the arm. At the level of the boards the connectors ensure the cabling dispatching inside the cryostat allowing the motion of the rotating arm. All cables for the sensors are feed through a device, called moving adapter device or "pancakes", and then connected to feedthrough on the top flange of the cryostat.

Driving and Suspension Frame (DSF)

A total of 116 surface scanning thermometers¹³ and 32 photodiodes are assembled into 9 rotating arms which are mounted in the DSF as shown in Figure 3. The most important consideration in the mechanical design is to assure the three dimension tolerance between the cavity surface and the tips of the 116 thermometers over entire cavity surface (i.e. more than 10,000 points) within ± 1 mm. The DSF has two centring

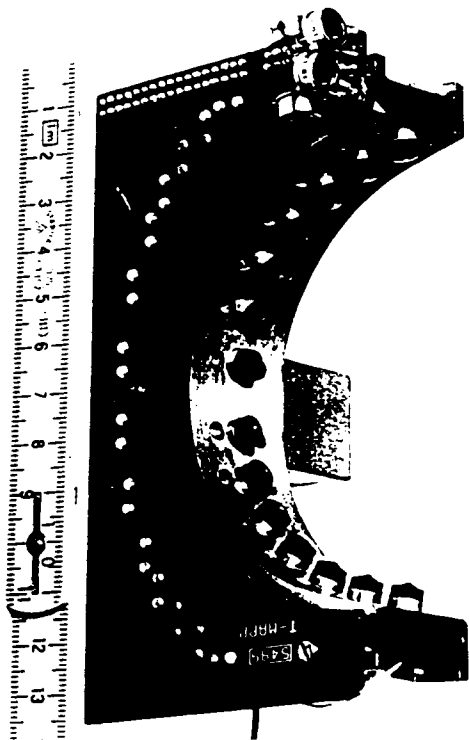


Figure 2. A picture of the rotating arm.

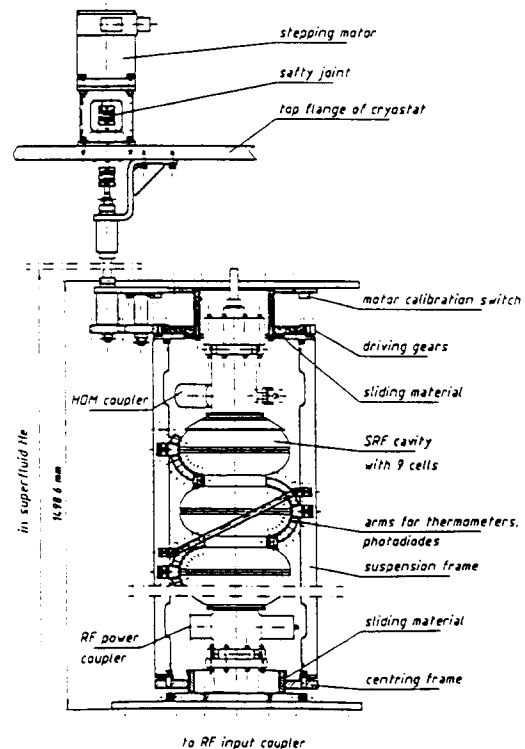


Figure 3. A cross section of the DSF

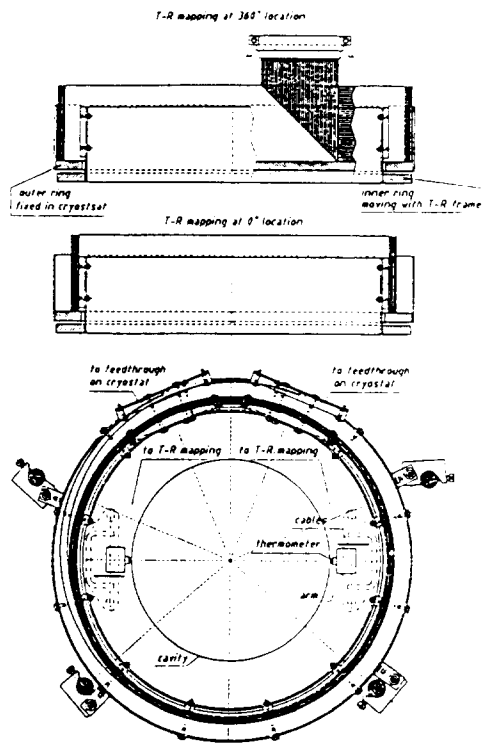


Figure 4. A schematics of a MAD

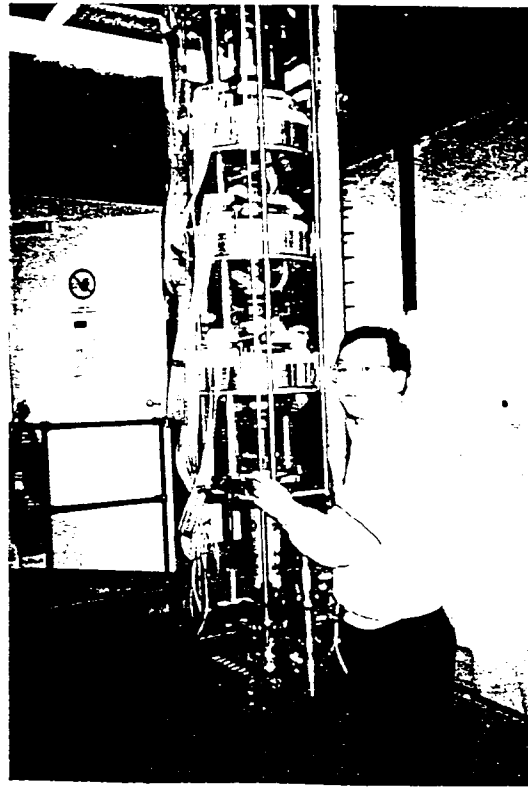


Figure 5. A complete T-R mapping system

rings to allow the axis of DSF as close to the axis of cavity cells as possible. The rotating frame is also suspended on two disks made of low fraction materials at low temperature. These structures enable the DSF in superfluid He to gently turn the arms around the cavity and uniformly press the thermometers (through the spring-holder structure, $P=100$ g per thermometer) against the cavity surfaces. Driven by a computer-controlled stepping motor, the T-R arms can be automatically turned to any suspect position on the cavity surface with a accuracy of ± 1 degree.

Moving Adapter Device (MAD)

A large number of electronic measuring cables have to move with the rotating arms when the T-R mapping rotates. These cables become very rigid in LHe. A moving adapter device¹³ was successfully designed to overcome the problem as shown in Figure 4. Each pancake has two rings. The inner ring is mounted in the moving DSF and turns with the DSF around the cavity. Its outer ring is fixed with cavity supports. One end of each 64-wire-cable is connected to the inner moving ring and the cables make 9 turns around the inner ring of the MAD while the another end of the cables connects to the outer fixed ring. When the DSF turns 360° around the cavity, the cables only make relatively short movement inside the MAD. The space in the TTF vertical cryostat is very constrained which makes the MAD design even more difficult. As shown in Figure 4, the MAD has been tested and functions well in many cavity experiments. Figure 5 shows the complete T-R mapping system.

Fast Data Acquisition and Test Procedure

Two Ge-thermometer and three additional scanning thermometers are used to monitor the change of bath temperature during measurement. To check the photodiodes two small lights are placed in the DSF. Maps can be taken with auto-scanning of entire cavity surface or scanning with time in a fixed position. The temperature change ΔT is made by comparison of two measurements of RF power on and off (also, the bath temperature changes are subtracted from the total ΔT). The effective resolution of temperature measurement is less than 5 mK. One longitudinal measurement in a fixed

language position on the screen. The data acquisition and control software are performed through a multiplexer by a Sun-station computer with a LabView™ language program [4].

RESULTS, ANALYSIS & DIAGNOSTICS

The T-R mapping has been successfully employed in the diagnostic testing of TESLA SRF cavities. We will briefly introduce some of the more interesting results here. A detailed test report will be presented in the "1995 SRF Superconducting Workshop".

Detection of Thermal Breakdown

We use the TESLA 9-cell cavity (D-6) as an example shown in Figure 6. This cavity has been heat treated with Ti-purification at 1400° C for 4 hrs and a monitory sample has a RRR of about 500. At first, the cavity was limited by severe FE at $E_{acc} = 4$ MV/m and Q dropped to 8×10^7 , Fig. 6 (A). With RF power processing, the FE events were eliminated and the T-maps show the heating areas by FE gradually disappeared. Finally the cavity reached $E_{acc} = 12.5$ MV/m through a high RF pulse peak power processing (HPP) and then limited only by a quench.

While scanning the entire surfaces of the 9-cell cavity, the T-mapping located a strong heating area centred at the equator of the cell-5 across over 10 thermometers in longitudinal between the 0° to 40° as shown in Fig. 6 (B). To further study the TB event, we relocated the T-R arm to the heating area, moved it by 5° angular stepping and found the hottest spot to be around 15°. Finally we moved the arms to the 15°, turned on the RF power in CW mode and observed continuing quenches of the cavity as shown in Fig 3 (C). Simultaneously, we continuously took the temperature measurements at the fixed location. Fig. 6 (D) show the temperature changes at 15° as a function of time. It also indicates the dynamic progress of the cavity quench in local area. The highest temperature measured on

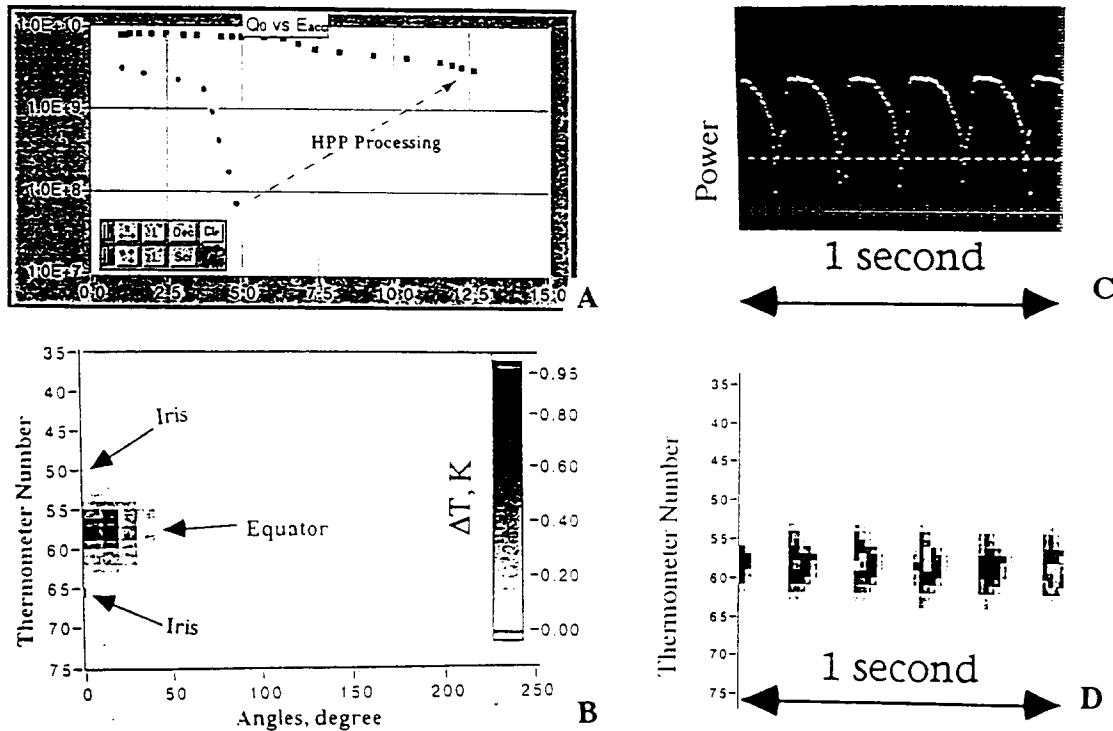


Figure 6. (A) overall RF performance of the TESLA 9-cell cavity D6. (B) The detected heating area due to TB at the equator of cell-5. (C) Oscilloscope traces of transmitted power during continuing TB of the cavity. (D) The temperature changes at longitudinal of 15° of the cell-5 during continuing TB of the cavity

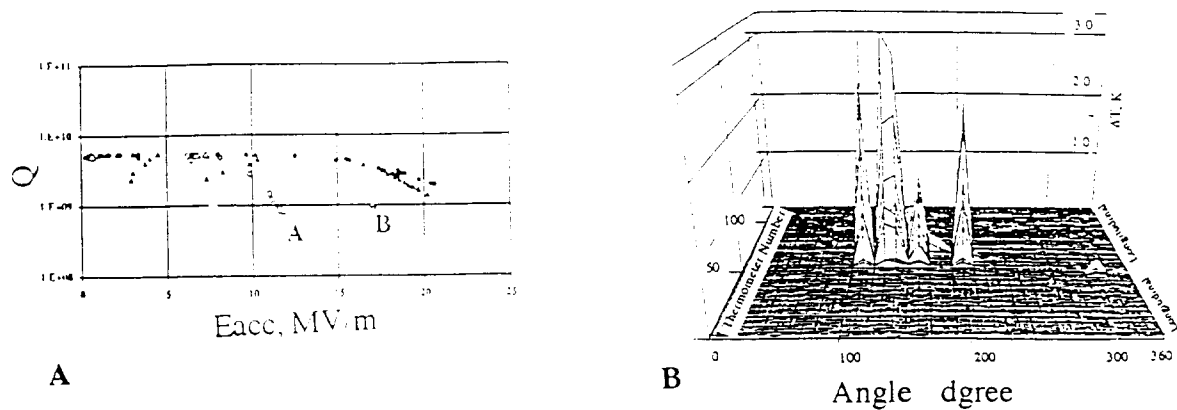


Figure 7. (A) Overall RF performance of the TESLA cavity -1. (B) Heating area responsible for the Q dropping and limit of Eacc

the outer surface of the cavity is above 5 K and the quench was limited in one cell and did not propagate to the adjacent cells.

These results indicate that HPP is very effective in elimination of FE¹⁵, but not for TB. The tests tell us that there may be a combination of local defects at cell-5 and existence of a low thermal conducting thin layer (due to Ti-purification) on the cavity. Optical observation after test showed a suspected deep scratch on the inner surface near the equator and close to 15° of cell-5. We are planning to take an additional 50 μm of material from the inner surface and re-test it again.

Identification of FE Heating and Emitter Location

In investigating FE, we first use T-R mapping to identify the landing areas of FE electrons and then find out the locations of emitters with simulations of FE electron trajectories. we use a TESLA prototype 9-cell cavity (-1) as an example. It has reached 20 MV/m as shown in figure 7 (A). Previously, cavity -1 had been limited by thermal breakdown at about Eacc = 10 MV/m. Afterwards, the cavity -1 was heat treated at 1400° C with Ti-purification. We then removed 80 μm of material from the inner RF surface and 30 μm from outer side by chemistry, followed by high pressure rinsing.

Locating of Heated Areas and Intensity

In the test the cavity -1 was initially stopped by heavy field emission at point A of 11.2 MV/m with a Q, 8.5×10^8 . The T-map, Figure 7 (B) indicate an important heated region delimited by 12 thermometers (#53 to #64) centred close to the equator of the 5th cell, between the 110° to 200° angles. Outside of this region the heating is very low. The ΔT value in this region is 100mK - 3.3K. The y-axial of figure 7(B) is the thermometer number from 0, close to the top iris of cell-1, to 116, close to the bottom iris of cell-9. The x-axial represents the angular location on the cavity surface.

Analysis of Thermal Performance

The experimental data obtained with the T-R mapping is consistent with the thermal analysis if we consider the following assumptions: high efficiency of thermometer at high heat flux, heat transfer governed by Kapitza regime, and electron trajectories impacts over a large area. The magnetic field heating at equators of the 5th cell, for Eacc=11.2 MV/m and Rs=30 nΩ, gives only ΔT=5 mK. The power related to the electron FE, Pelec=173 W, is focusing on local region.

The very high value ΔT measured in this region (100mK-3.3K) can only be explained by assuming that the efficiency of a scanning thermometer increases strongly with the heat flux density at the interface of cavity wall and HeII. Such a high heat flux density is

slightly less than the critical heat flux densities reported in experiments with metallic flat heaters in HeII¹⁶. So it is believed that the heat transfer is in the regime governed by Kapitza conductance. The integration of the product of Kapitza conductance and ΔT over the heated region leads to a total heat power going to He bath: $Q \sim 100$ W. This value is consistent with the RF measurements of the experiment.

Identifying of FE Emitter Location

Locating origins of FE and TB is very important to understand the influence of various cavity processing and also to a guided reparation of defected cavities. However, the measured hot spots only indicate the landing of impacting FE electrons, but not the emitter.

The simulation of FE electron trajectories demonstrate the following interesting results: FE electrons from an emitter can impact over a very large area, the shape of trajectories are sensitive to emitter location (S_o), and an emitter responsible for the heating shown in figure 3 is successfully identified. Since electron trajectories, impacting electron energy and power deposition distribution (dP/ds vs. s) are controlled by the E_{acc} and S_o , a series of simulations are performed by changing S_o at $E_{acc} = 11.2$ MV/m, assume $b = 200$, S_e (emitter area) = 1×10^{-13} m². It is found that an emitter located at $S_o = 8$ cm (at the iris area in a curvilinear co-ordination) has electron trajectories shown in figure 8 A. Its power distribution (dP/ds vs. s) in Figure 8 B seems to be very close to the shape of the measured temperature distribution 8 C. It is indicated that heated areas at the equator (usually by defects) can also be caused by FE. The b and S_e (emitter area) of the candidate emitter were adjusted to fit with the thermal analysis and RF experimental data. For instance, at $E_{acc} = 11.2$ MV/m, if $S_e = 1 \times 10^{-13}$ m², $b = 400$, the total mean power landed over RF period is 10W.

Finally, the high pulse RF power processing (HPP) was introduced to the cavity (150KW) and successfully eliminated the field emitters. Another T-map also witnessed the FE elimination. After HPP, the cavity finally reached 20 MV/m in cw mode.

Information from X-Ray Maps

A large number of radiation maps of X-rays induced by FE electrons were also observed. In general, information from X-ray maps are in consistent with that obtained from T-maps. As we mainly discuss the technical areas relevant to low temperature

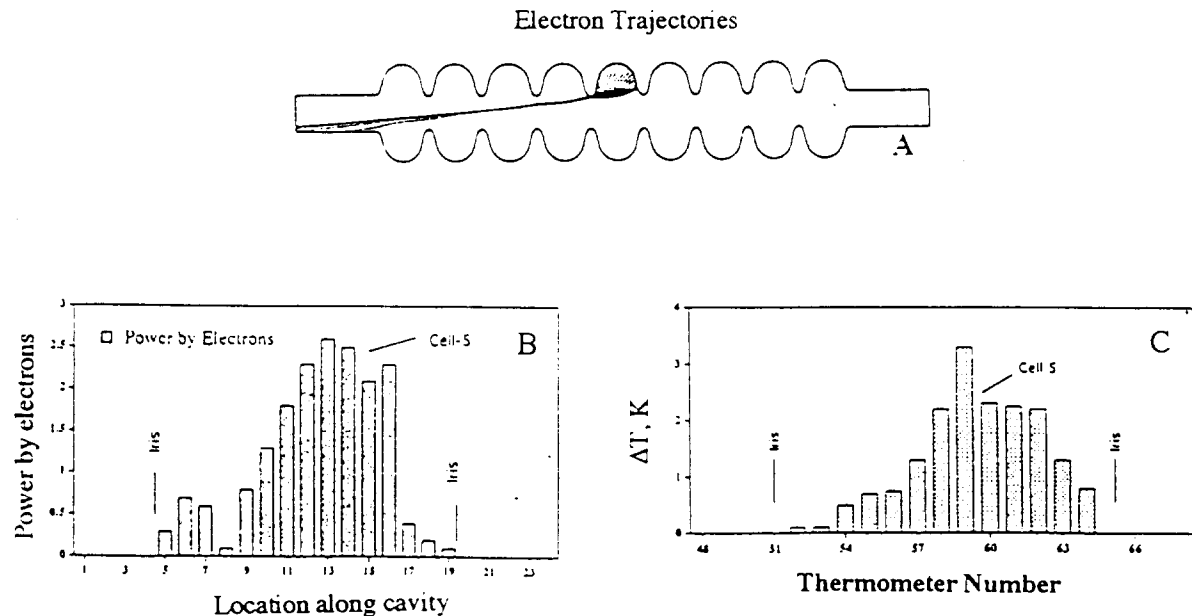


Figure 8. (A) FE electron trajectories of the emitter located at $S_o = 8$ cm and the emitter is responsible for the Q degradation. (B) Power distribution contributed by impacting FE electrons from $S_o = 8$ cm. (C) experimental longitudinal ΔT plot from T-map data of Figure 7 B fixed at 140°.

science here, the X-ray maps and analysis will be presented at the 1995 SRF superconducting workshop (Saclay, France).

CONCLUSION

The T-R mapping system for TESLA 9-cell cavities was commissioned and successfully analysed and diagnosed the problems with the TESLA cavities caused by FE and TB. The information learned from T-R mapping results has played a significant roles in cavity processing and will be very valuable in further guided reparation of some cavities.

ACKNOWLEDGEMENT

We sincerely thank P. Kneisel (CEBAF), W. Weingarten (CERN), H. Padamsee, M. Champion (Fermilab), C. Pagani (INFN), B. Bonin (Saclay) and G. Wueller, R. Roeth (Wuppertal) for many fresh discussions and hints. Sincere thanks are also presented to our DESY colleagues in the cryogenic group, vacuum group, mechanical group, MHF group for their support.

REFERENCES

1. D. Proch: Proc. - 5th workshop on RFS, DESY, 1991.
R. Sundelin: Proc. - 6th workshop on RFS, CEBAF, 1993
2. H. Pademsee, Applied Supercond. Conf., Boston, 1994.
3. Q.S. Shu et.al., IEEE transaction, Vol. 27, No. 2, 1991
4. B. Bonin et. al., Proc. of 6th workshop on RFS, 1993.
5. R. Roth and G. Muller et. al., Proc. of the 5th (and 6th) workshop on RFS, DESY 1991 (and CEBAF, 1993).
6. Ph. Bernard et. al, Nucl Inst & Met in Phys Res vol 190
Ph. Bernard et. al. & S. Buhler et. al, the 5th (and 6th) workshop on RFS, DESY 1991 (and CEBAF, 1993).
7. Q.S. Shu et.al., Nucl Inst & Met in Phys Res A278. 1989.
J. Knobloch, et. al., SRF 94-0419-03, Cornell Univ., 1994
8. M. Fouaidy et al Proc 5th workshop on RFS, DESY, 1991.
9. T. Junquera et. al. TTP 14, Dallas, TX. PAC/95.
10. Q.S. Shu. et. al., TTP 19, Dallas TX. PAC/95.
11. R. Romijn, W. Weingarten, IEEE Trans. on Magnetics, Mag 19 (1983), p. 1318,
12. S. Buehler, et. al., workshop on RFS, CEBAF, 1993
13. Q. S. Shu, et al. TESLA internal presentation, February, 1995
14. M. Pekeler, TESLA internal report
15. J. Graber et. al., Nucl Inst & Met in Phy Res A278. 1989.
16. A. Kashani, S. W. Van Sciver. Cryogenics 25, 1985